EXPERIMENTAL AND NUMERICAL PREDICTION OF VELOCITY AND TEMPERATURE FIELDS IN A ROOM HEATED BY A ROOM AIR-CONDITIONER

H.HANIBUCHI, S.HOKOI, Ph.D.

ABSTRACT

One of the great influential feature on room temperature distribution is the insulation quality of the room. Each room of the typical Japanese modern house has a low heat capacity, high insulation quality and large windows which are less insulated. Temperature near the window is naturally low. These factors make the thermal insulation of the room strongly uneven. When heating the room, the location of the heat source largely affects room temperature distribution as well. This kind of distribution will be emphasized using an air-conditioner. Room air temperature using heating equipment such as this has both a high temperature area due to the air jet discharged from the outlet and several low temperature areas due to drafts from the window. Such a wide temperature distribution does not contribute to the comfort of the occupants at all. On the other hand, the location of the heat source also influences the heat loss of the room. Thus, an appropriate location for the heat source will produce good thermal conditions and save on heating energy.

In this paper, the distribution properties of room air temperature, velocity and heat loss are discussed experimentally and analytically. Measurements under heating condition were made in a full-scale model room in order to investigate the influence air-conditioner location has on velocity and temperature fields in a steady state, as well as heat load. The following results were obtained: (1) the influence of the direction in which the jet was blown from the air-conditioner was clearly seen in regions of different temperature distribution adjacent to the floor; (2) the heat loss calculated from these experimental results show several differences characterized by the direction of the blown jet and the difference between the maximum and minimum heat loss obtained from these four experimental results is roughly 15%; and (3) results from numerical analyses agree with experimental results.

KEYWORD

Room airflow, Temperature distribution, Heat load

Haruo HANIBUCHI is a Environmental Design Engineer, Institute of Building Science, SEKISUI HOUSE, LTD., Kizu, Kyoto 619-02, JAPAN. **Shuichi HOKOI** is a professor; Department of Architecture, Faculty of engineering, Kyoto University, Sakyo, Kyoto 606, JAPAN.

INTRODUCTION

It is not easy to keep room temperature uniform, even in a small space, using an air-conditioner because of inside air currents and drafts from windows which are less insulated than other structural constituents. Air flow and temperature distribution are strongly influenced by the location of windows and the air-conditioner. The consequential thermal condition, which has a wide distribution influenced by the factors mentioned above, is not appropriate for human comfort at all. Therefore, it is important to determine the best location for the air discharge outlet - in other words the location of the air-conditioner itself - in order to keep appropriate indoor air temperature in a typical room in the home. Since heat loss will be also influenced by the location of windows and the air-conditioner as well, the best location for the air-conditioner should be determined in view of energy saving.

Much research has been directed at room air flow and temperature already. For example, Kato et al. (1995) and Murakami et al. (1995) experimentally and numerically examined the thermal environment in a room cooled with a cooling jet and cooling panel. Takemasa et al. (1992) investigated new boundary conditions for simulating convective heat flux. This paper examines air flow, temperature field and heat load from yet another point of view: the influence borne by the location of the air-conditioner. Experiments were carried out in a full-scale model room using four different locations for the air conditioner. The influence of outlet location on temperature and heat load was evaluated from the obtained data. Several numerical analyses were also made and their validity was examined.

EXPERIMENTAL PROCEDURE

Experiments were carried out in a model room (Hanibuchi et al. 1996), schematically shown in Figure 1. This full-scale room was built inside a large climate chamber kept at a constant temperature of 2 °C. The experimental conditions are given in Tables 1 and 2. The values given in Table 1 were estimated from the respective structural materials used for preparing the room. Although the conditions and structure of the room in the experiment are not universal, discussion will be made the results at steady state so that the heat capacity may not need to be considered The air-conditioner itself, which is a Japanese-unique system, is one of the representative systems of force-convective heating. The steady state heat load was 1.84 kW, when the difference between the outside and inside temperature was set at 20 centigrade. Figure 3 illustrates where the air-conditioner shown in Figure 2 was located in the room. Measurements were carried out with the air-conditioner located in four different places. The difference in location is indicated as Cases 1 ~ 4 in Figure 3. Room air temperature, inside wall surface temperature and temperature at the air-

conditioner's outlet/inlet were measured by T-CC thermocouples, while both airflow in the room and at the outlet/inlet were measured by anemometers as shown in Table 3. The thermocouples on the wall were covered with an air-permeable seal which was almost the same color as the wall surface. Since sensors on the wall surface could measure radiative heat flux equally as well as convective heat flux, the obtained surface temperatures were regarded as the actual wall surface temperature. Air temperature was measured without anything covering the sensor. Temperature was measured in 55 points at a height of 50 mm and 600 mm above the floor. Room temperature was controlled by a remote controller and was set at 2°C. Therefore, the difference between indoor and outdoor air temperatures was approximately 20°C.

NUMERICAL PROCEDURE

In this part of the study, numerical analysis was applied to the measured temperature field and heat load. The results obtained by the following procedure will be discussed later with the experimental results. Three-dimensional numerical analysis was carried out for each Case using the k-ε turbulence model shown in Table 4. The set of boundary conditions shown in Table 5 were used in this study (Hanibuchi et al. 1996). The inside film coefficient at each cell adjacent to the wall was given the equation (3) in Table 5 using the combined velocity of the two components parallel to the wall at the same cell. These boundary conditions have been chosen after several numerical tests referred to in previous studies (Launder 1988, Murakami et al. 1995, Yurges 1924). Boundary conditions at the outlet and the inlet are also listed in Table 5. Fig. 4 illustrates a computer matrix of the plan and the section of the model room. For each calculations, measured values of inside surface temperature and that of outlet temperature and velocity were used for the boundary values for each computational cell. Thus, the room air temperature and velocity and inlet temperature, can be obtained as a set of numerical results. Radiative heat transfer analysis was not considered in calculations because it dose not have any contribution to the calculated result of heat load using the numerical conditions here, but it will be considered in the next step when heat exchange on the inside surface is examined in detail,

RESULTS AND DISCUSSION

Temperature distribution across horizontal plane

Figures 5 through 8 illustrate experimental temperature distribution across horizontal planes 50 mm and 600 mm above the floor, for the four different locations of the air-conditioner

(illustrated by black square in Fig. 3). Under these conditions, the jet from the air-conditioner produced a high temperature spot, indicated by the black arrow. At 600 mm, the average air temperature across the entire plane was almost the same in all Cases. It should be noted that, on the 600 mm horizontal plane, air temperature near the window was higher than that was expected. In general, temperature distribution, particularly on the lower horizontal plane, was significantly affected by airflow pattern. For instance, as shown in Figures 6 (Case 2, a) and 8 (Case 4, a), the air-conditioner supplied much of the warm air to only a part of the perimeter zone rather than to the interior zone. Cold air flows down to the floor near the window without receiving much warm air supply. When the air-conditioner was set at the center of a span wall, the interior zone was sufficiently heated as shown in Figures 4 (Case 1, a) and 7 (Case 3, a), although the temperature in the perimeter zone near the window was slightly low. In the results of Case 1 and 3, the high temperature region was slightly pushed aside from the center of the room although the jet was discharged straight from the outlet. This fact can be seen in the velocity result as mentioned later.

The numerical temperature results across a horizontal plane 50 mm and 600 mm above the floor are shown in Figures 9 through 12 along with the experimental result of each of the four Cases. The numerical results give reasonable distribution features in each Case. However, the calculated temperature is lower than the experimental result for the most part in all Cases. The difference between the two results is mainly due to the film coefficient used in calculations. The value of the film coefficient used in these calculations is variable by calculated velocity near the boundary. Thus, temperature results are influenced by the velocity. Although several further estimations must be conducted to conclude that the difference between the numerical and experimental results is mainly due to the constant coefficients in the film coefficient formula or the velocity result itself, it can be regarded that the film coefficient was overestimated in calculations. Numerical results obtained here, however, agree fairly well with experimental results. For example, the numerical results of Case 1 and 3 predict the experimental fact that the high temperature region was slightly pushed aside from the center of the room.

Velocity distribution across horizontal plane

The scalar velocity distributions across a 200 mm horizontal plane for Case 1 and Case 2 are shown in Figure 13. Because velocity near the wall was not measured in Case 1, these area are omitted in the contour. The high velocity area; example for where the velocity is over 0.6 m/s, reasonably fits to the high temperature area (see Fig. 5 and Fig. 6), though the low velocity area dose not perfectly fit to the low temperature area. As mentioned before, in the result of Case 1, the high temperature region in Figure 5 was slightly pushed aside from the center of the room. This corresponds to the velocity result in Figure 13 (a) where the high velocity region was slightly pushed aside from the center of the room. The result suggests that the jet air from the outlet blows away from the window as if the jet air was forced to be curved by the down draft from the windows.

Numerical scalar velocity distributions across a horizontal plane 200 mm above the floor are also shown in Figure 14 for Case 1 and 2. These two numerical results agree with the experimental velocity distribution including the experimental fact that the high velocity region was slightly pushed aside from the center of the room. In Case 2, numerical result agree well with the experiment near the boundary.

Vertical temperature profile

Vertical temperature profiles are shown in Figure 15 as a comparison between the experiment and calculation for each of the 4 Cases. The average value across the entire plane was used to plot the profile for each height. The most notable feature is that measured values in the upper position more than 1800 mm high from the floor are similar in all Cases, whereas, that in the lower position less than 600 mm high from the floor are greatly different. This is one of the great influences of the location of a heat source when force convective heating equipment is used. The calculated temperature is lower than the experimental result in all Cases, however their profile agree well with experimental results as mentioned above.

Velocity profiles

Calculated velocity profiles obtained for Cases 1 and 2 are compared with measured data in Figures 16 and 17. Line X-200 indicates the center line of X span at 200 mm height above the floor and Line X-120 indicate the center line of X span at 1200 mm height above the floor. The same representations were used for Y-200 and Y-1200. The number of measured point is small, however, calculated result are agree well with experiments. These facts seem to point out that the thermal boundary condition, thus the estimation of film coefficient in this study, significantly influences the temperature field but not the velocity field.

Heat loss

Table 6 shows both experimental and numerical temperature results at the inlet and outlet. As mentioned in the numerical procedure, the outlet temperature in calculations is the same as measured values. The supplied air volume was calculated from the velocity distribution of an outlet jet, based on several measured values. The heat supplies in Table 6 were obtained from the temperature difference between the outlet and the inlet, and the supplied air volume, as mentioned above. Table 7 shows the amount of heat loss in walls, floor and ceiling obtained by experiment and calculation. These experimental values were calculated based on the difference between temperature measured on the inside surface of the walls and outdoor temperature, and the amount of conductance between them.

$$Q = \Sigma\, q_i\, S_i \qquad (1)$$

$$q_i = D_m(T_w - T_o) \quad (2)$$

$$R_m = 1/D_{im} = r_w + 1/\alpha_o \quad (3)$$

wherein;

Q = total heat loss [W]

q_i = heat flux at *i* th cell [W/m^2]

D_m = thermal conductance between inside surface and outdoor temperature [W/m^2K]

S_i = square of *i* th cell [m^2]

T_w = inside surface temperature of *i* th cell [°C]

T_o = outdoor temperature [°C]

R_k = thermal resistance of *i* th wall (windows etc.) [mK/W]

r_w = conductive resistance of *i* th wall (windows etc.) [mK/W]

α_o = film coefficient outside [$W/m^2 K$]

The difference between outlet and inlet temperature was almost the same in all four Cases as shown in Table 6. Total heat loss in Table 7 was almost equal to the heat supply in Table 6. Slight differences between the heat supply and loss observed in Case 2 and Case 3 are within the acceptable uncertainty range. Wall 1 and Wall 3 had windows as shown in Figure 1. Most of the heat was lost through windows. The largest amount of heat loss occurred in windows 2 and 3 for Case 2 and in window 3 for Case 4. This is because the high temperature jet from the outlet flowed across the window.

The calculated heat loss is larger than experimental result in all Cases. This result can be attributed mainly to the film coefficient used in calculations being slightly overestimated. This must be the reason why the calculated average room temperatures are slightly lower than that in experiments. The difference between the calculate and experimental heat loss, however, is within 9 % in all Cases, which is acceptable.

Since the obtained averages room air temperatures from experiment not equal in each Case as shown in Table 6, it is impossible to estimate the influence outlet direction had on heat load exactly. Therefore, each of the values in Table 7 was recalculated by normalizing the average room air temperature as 22°C and outdoor temperature as 2°C using the following equations (4) and (5) instead of equations (2) and (3). The detailed description of equation (4) is given in the appendix.

$$q_i = K'(T_r' - T_o') \quad (4)$$

$$K' = \frac{1}{r_o + r_w + \frac{T_i - T_w}{T_w - T_o}(r_w + r_o)} \quad (5)$$

wherein,

K' = overall heat transfer coefficient [$W/m^2 \cdot K$]

T_i = average room air temperature measured for each Case [°C]

T_w= inside wall surface temperature of *i* th cell measured for each Case [°C]

T_r' = average room air temperature (= 22°C)

T_o' = outdoor air temperature (= 2°C)

The normalized heat losses calculated in this way are shown in Table 8. An ignorable difference can be seen in the heat loss through the window. In Case 2, the heat loss through Walls 2 and 3 is larger than that of other Cases, whereas, the heat loss through Wall-1 in Case 4 is largest of all cases. This must be a major reason for the difference between the maximum and minimum normalized heat load being more than 10%. This fact shows that different levels of energy consumption may be required in order to make the room temperature equal in all cases. The result of Case 1 is desirable in view of the savings on heating energy.

CONCLUSIONS

Measurements under heating condition were made in a full-scale model room and the influence air-conditioner location has on velocity and temperature fields in a steady state, as well as on heat load, were investigated. Several numerical analyses were also applied. The following remarks are obtained as conclusions.

(1) The influence of the direction in which the jet was blown from the air-conditioner was clearly seen in regions of different temperature distribution adjacent to the floor.

(2) The heat loss calculated from these experimental results show several differences characterized by the direction of the blown jet and the difference between the maximum and minimum heat loss obtained from these four experimental results is roughly 15%.

(3) The results from numerical analyses agree with experimental results.

REFERENCE

Hanibuchi, H.; Hokoi, S. 1996. Analysis of velocity and temperature fields in a room heated by a room air-conditioner. Proceedings of 5th International Conference on Air Distribution in rooms, ROOMVENT '96, Vol.1, pp. 445-452.

Kato, S.; Murakami, S.; Sato, M.; and Nakatani, Y. 1995. Experimental study on thermal environment in a room with cooling jet and cooling panel (Part 1). Transactions of the Society of Heating, Air-Conditioning and Sanitary Engineers of Japan, No.57, pp.93-103.

Launder, B.E. 1988. On the calculation of convective heat transfer in complex turbulent flows. J. Heat Transfer, Vol.110, pp.1112-1128.

Murakami, S.; Kato, S.; Kondo, Y.; Takahashi, Y.; Dongho, D. 1995. Numerical study on thermal environment in air-conditioned room by means of coupled simulation of convective and radiative heat transport (Part 1). Transactions of the Society of Heating, Air-Conditioning and Sanitary Engineers of Japan, No.57, pp.105-116.

Takemasa, Y.; Kurabuchi, T.; Kamata, M. 1992. Numerical simulation of indoor air temperature and wall heat flow distribution of a heated and cooled room. Proceedings of ISRACVE, ASHRAE, pp.99-107.

Yurges, W. 1924. Der Warmeubergang an einer ebenen Wand. Beihefte zum Gesundheits Ingenieur, Beiheft 19. pp.1-51.

APPENDIX

At the steady state, temperature gradient is liner to the thermal resistance and heat flux at any point is constant. It supposed to be the same condition in a series of experiments here, thus, following relation can be obtained.

$$\frac{T_w - T_o}{r_w + r_o} = \frac{T_i - T_w}{r_i} \qquad \text{(A1)}$$

wherein, T_w [?] , T_o [?] and T_i [?] are the measured temperatures at inside wall surface, that of outdoor air and average room air respectively. Likewise, r_w [m^2K/W] and r_o [m^2K/W] are the thermal resistance of the wall (and windows, etc.) and combined outdoor heat transfer resistance, whose values are used in experimental analysis. The film resistance for inside surface represented by r_i can be obtain as the following formula.

$$r_i = \frac{T_i - T_w}{T_w - T_o} (r_w + r_o) \qquad \text{(A2)}$$

And overall heat transfer coefficient K' [W/m^2K] can be reduced.

$$\frac{1}{K'} = r_w + r_o + \frac{T_i - T_w}{T_w - T_o} (r_w + r_o) \qquad \text{(A3)}$$

Thus, the normalized heat flux q_i[W] for each point can be calculated by the following.

$$q_i = K'(T_r' - T_o') \qquad \text{(A4)}$$

wherein, T_r' is average room air temperature and T_o' is outdoor air temperature. Each value of T_r' and T_o' is 22 °C and 2°C respectively.

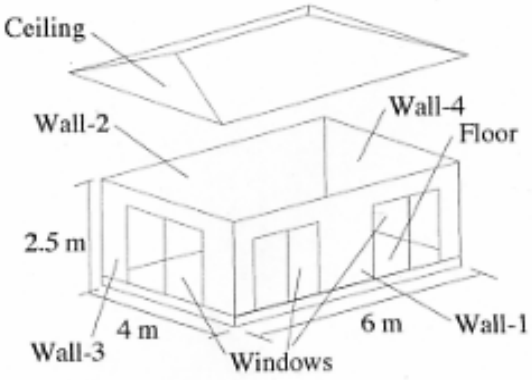

Figure 1. View of the model room set in a climate chamber.

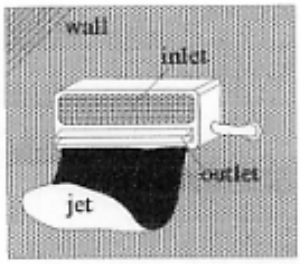

Figure 2. Illustration of air-conditioner.

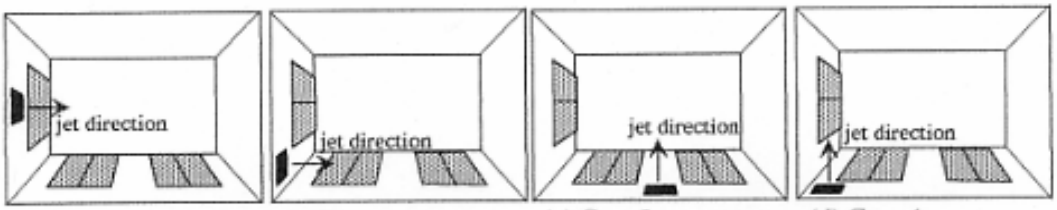

(a) Case1. (b) Case 2. (c) Case 3. (d) Case 4.

Outlet jet blows onto a floor in the direction of an arrow.

Figure 3. Position of air-conditioner for each experiment.

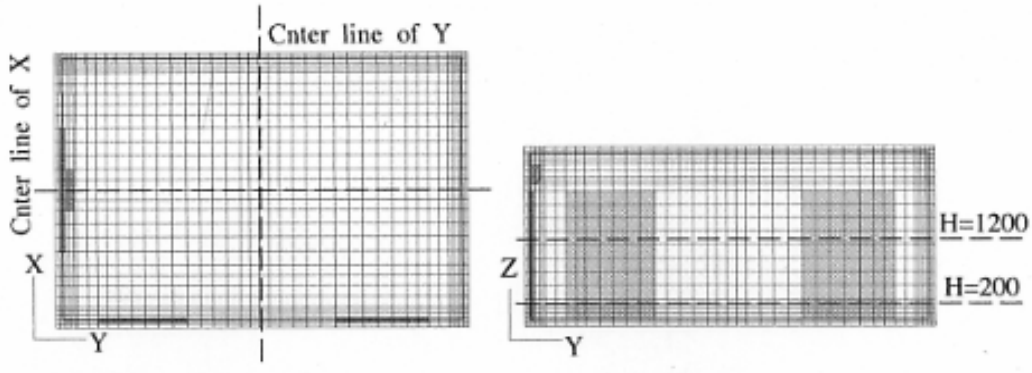

(a) X-Y Plan (b) Y-Z Section

Figure 4. Computer matrix was divided into 28×38×22 meshes.

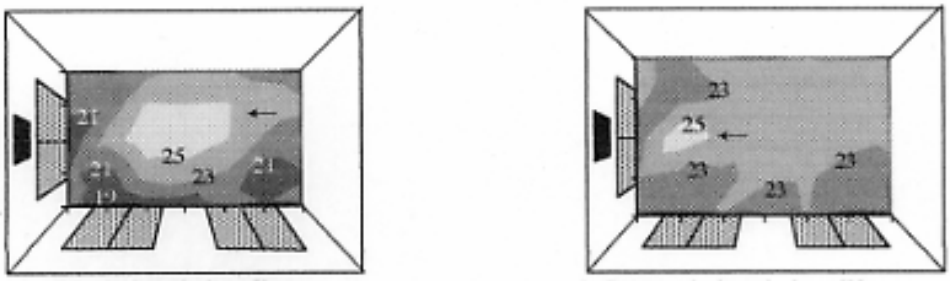

(a) Contor at horizontal plane 50 mm. (b) Contor at horizontal plane 600 mm.

Characteristic high temperature spot produced by an outlet jet is indicated by an arrow. Black & white numbers represents temperatures (℃).

Figure 5. Temperature distributions (case 1).

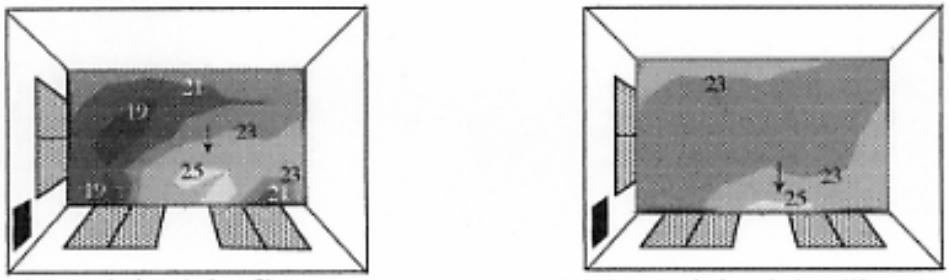

(a) Contor at horizontal plane 50 mm. (b) Contor at horizontal plane 600 mm.

Characteristic high temperature spot produced by an outlet jet is indicated by an arrow. Black & white numbers represents temperatures (℃).

Figure 6. Temperature distributions (case 1).

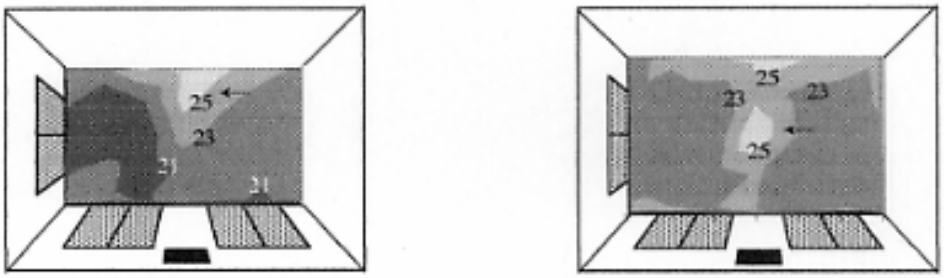

(a) Contor at horizontal plane 50 mm. (b) Contor at horizontal plane 600 mm.

Characteristic high temperature spot produced by an outlet jet is indicated by an arrow. Black & white numbers represents temperatures (℃).

Figure 7. Temperature distributions (case 1).

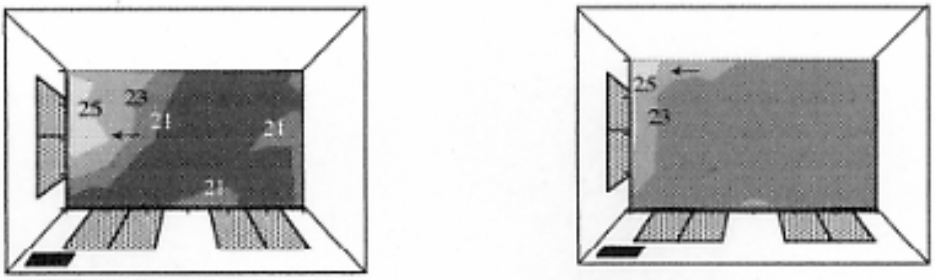

(a) Contor at horizontal plane 50 mm. (b) Contor at horizontal plane 600 mm.

Characteristic high temperature spot produced by an outlet jet is indicated by an arrow. Black & white numbers represents temperatures (℃).

Figure 8. Temperature distributions (case 1).

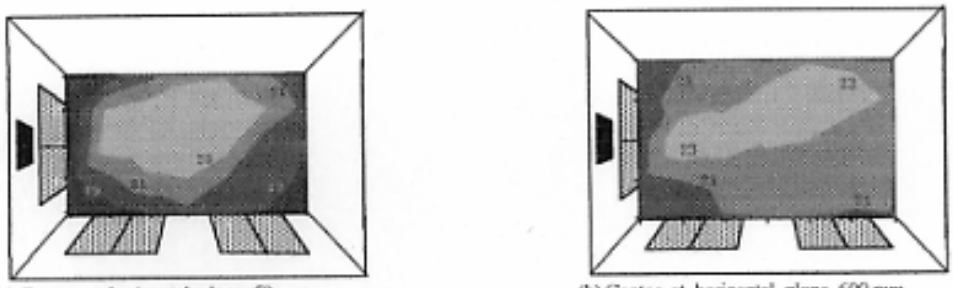

(a) Contor at horizontal plane 50 mm. (b) Contor at horizontal plane 600 mm.

Black & white numbers represents temperatures (℃).

Figure 9. Calculated temperature distributions (case 1).

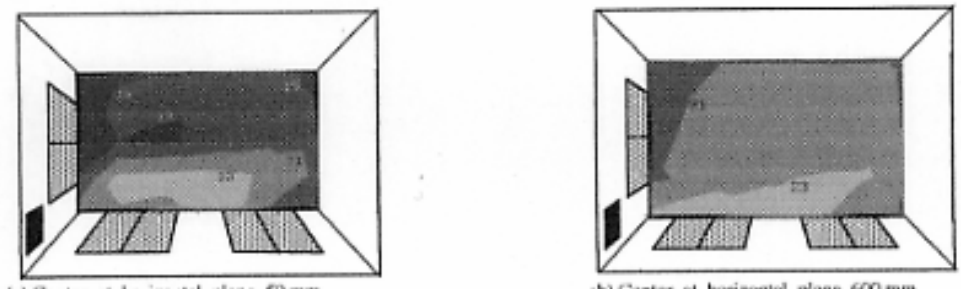

(a) Contor at horizontal plane 50 mm. (b) Contor at horizontal plane 600 mm.

Black & white numbers represents temperatures (℃).

Figure 10. Calculated temperature distributions (case 2).

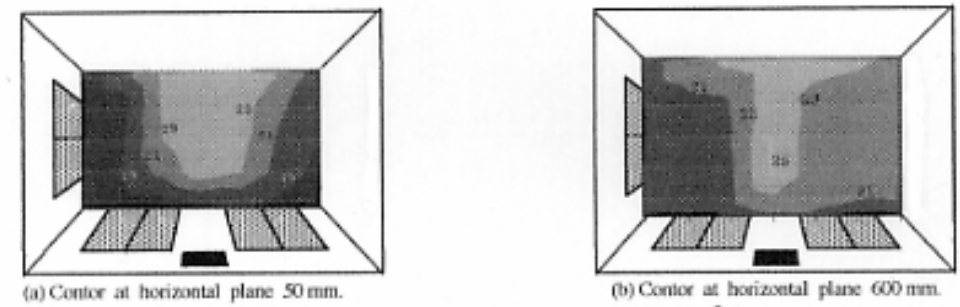

(a) Contor at horizontal plane 50 mm. (b) Contor at horizontal plane 600 mm.

Black & white numbers represents temperatures (℃).

Figure 11. Calculated temperature distributions (case 3).

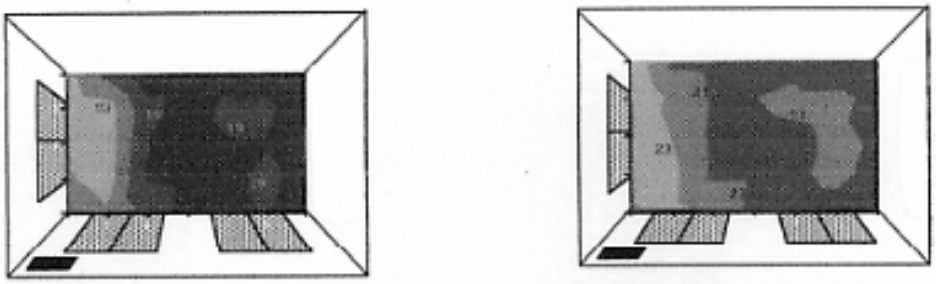

(a) Contor at horizontal plane 50 mm. (b) Contor at horizontal plane 600 mm.

Characteristic high temperature spot produced by an outlet jet is indicated by an arrow.
Black & white numbers represents temperatures (℃).

Figure 12. Calculated temperature distributions (case 4).

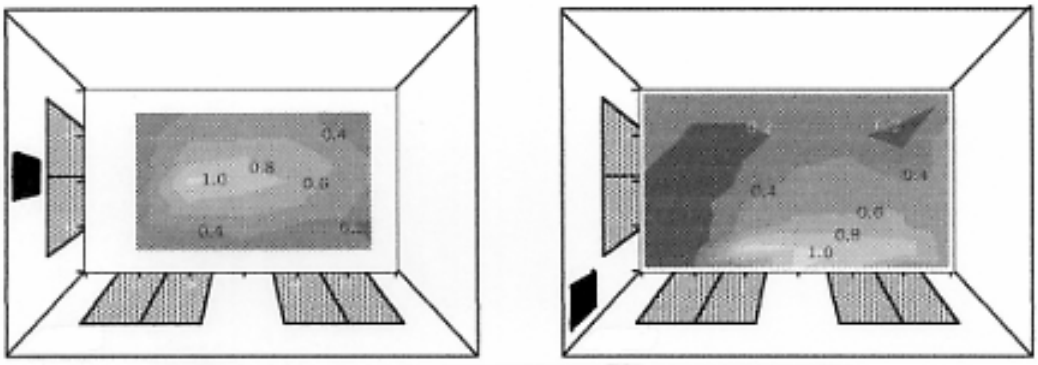

(a) Case 1 (b) Case 2

Black & white numbers represents velocity (m/s).

Figure 13. Measured scalar velocity distributions at 200mm height.

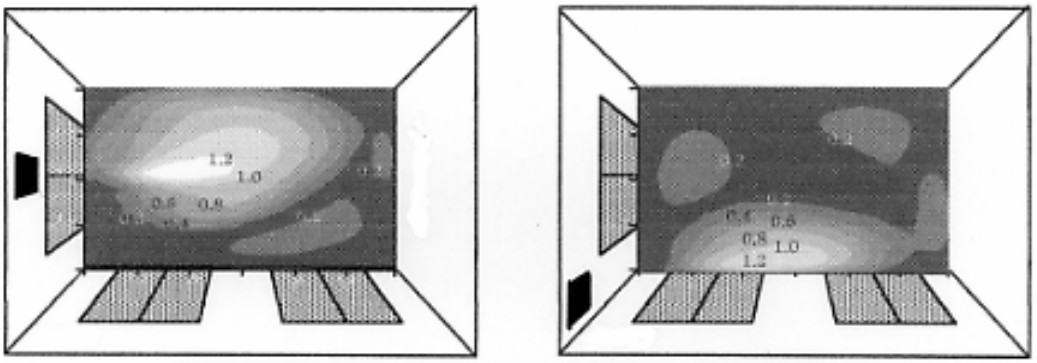

(a) Case 1 (b) Case 2

Black & white numbers represents velocity (m/s).

Figure 14. Calculated scalar velocity distributions at 200mm height.

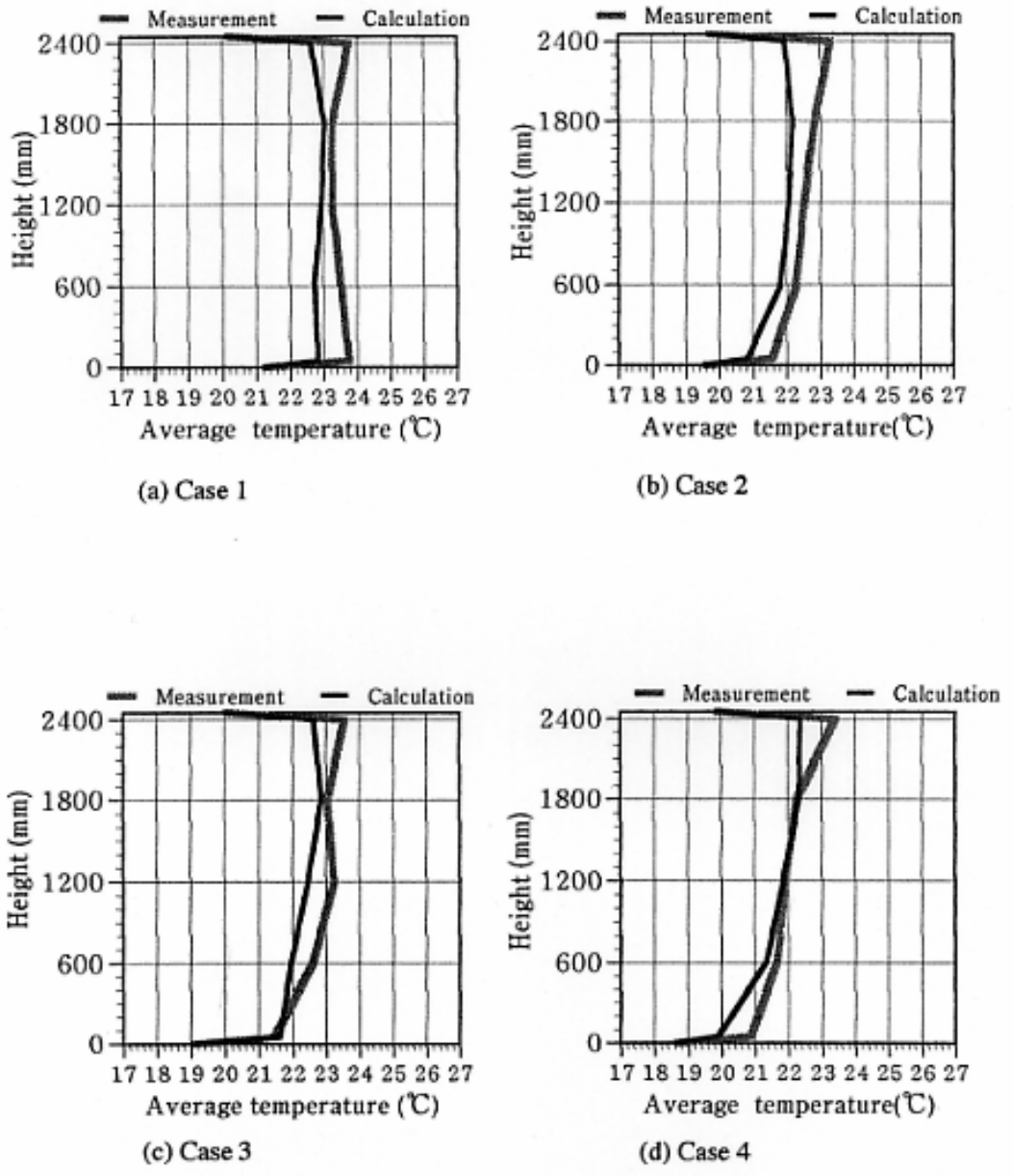

Fig15. Vertical temperature profiles

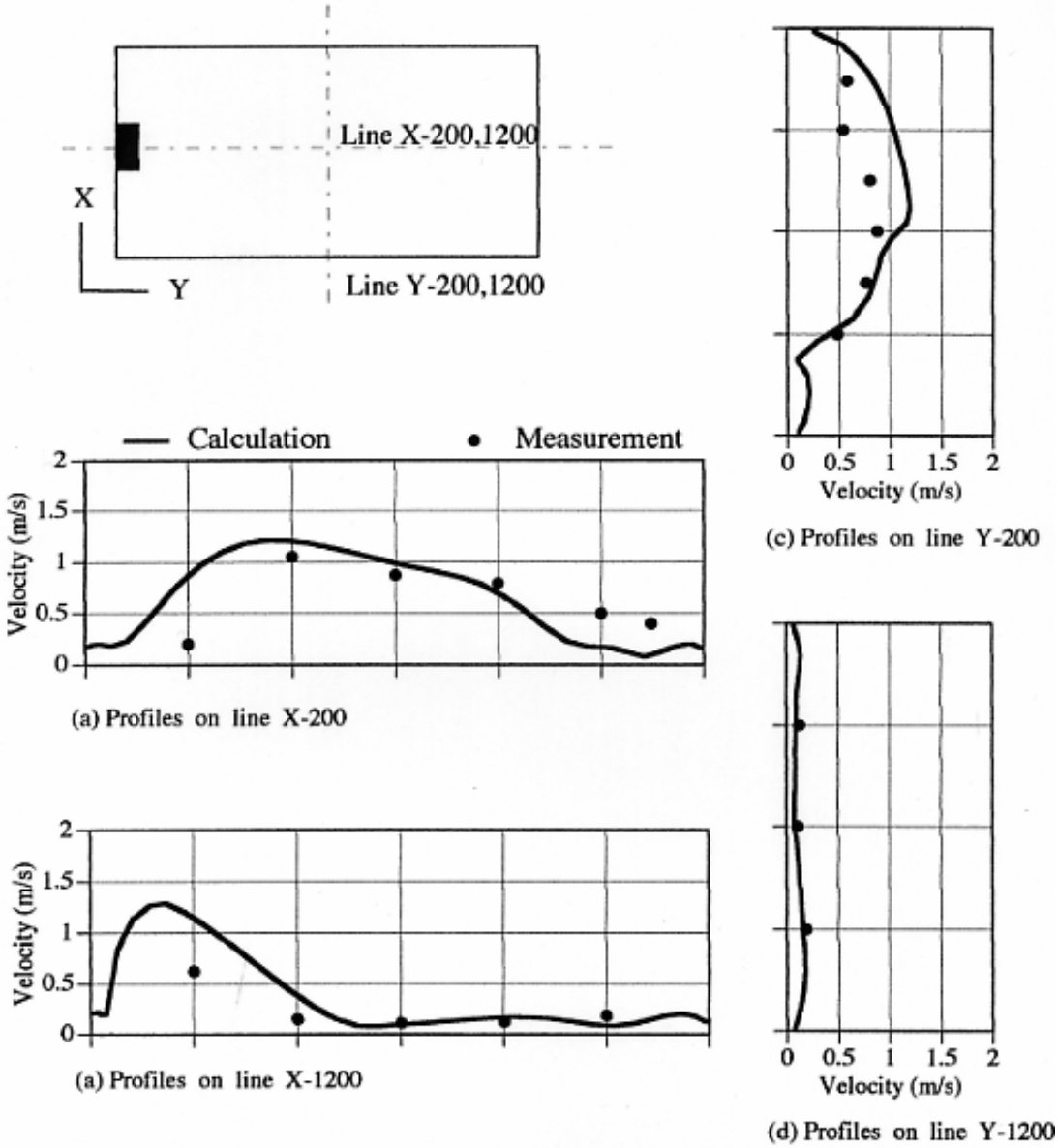

Figure 16. Mean velocity profiles (Case 1).

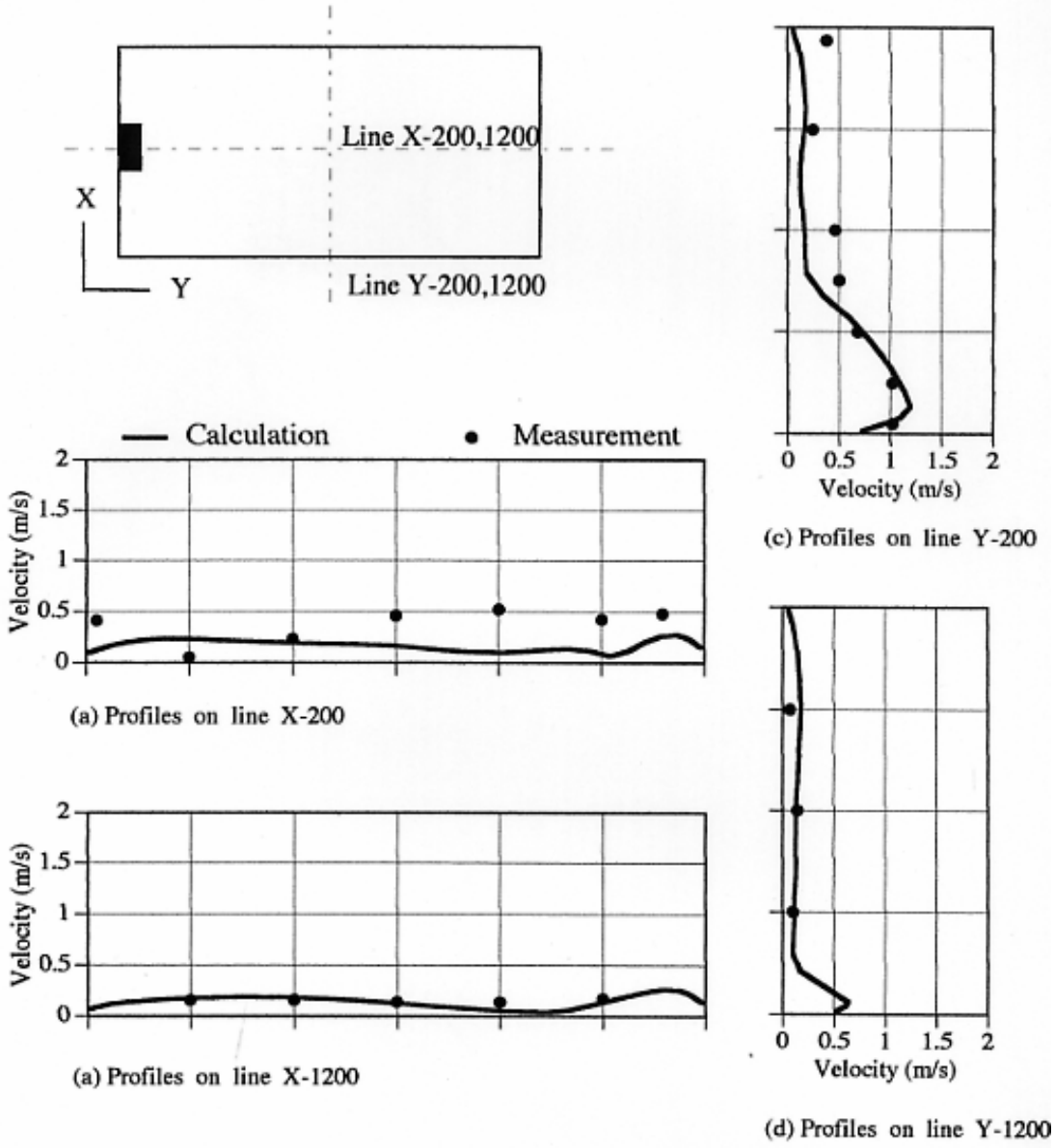

Figure 17. Mean velocity profiles (Case2).

Table 1. Thermal conductance.

Wall-1,Wall-3	0.55 W/m^2K
Wall-2,Wall-4	0.27 W/m^2K
Floor	0.60 W/m^2K
Ceiling	0.32 W/m^2K
Windows	4.51 W/m^2K

Table 2. Experimental conditions.

Outside temperature	275 K (2 ?)
Expected room air temperature	295 K (22 ?)
Solar radiation	none
Inside heat source	none
Inside obstacles	none
Occupants	none

Table 3. Measuring values.

Inside		
	Room air temperature (measured by thermocouple)	120 points
	Inner surface temperature (by thermocouple)	210 points
	Mean airflow velocity (by anemometer)	15 points
Others		
	Outlet/Inlet temperature (measured by thermocouple)	
	Outlet/Inlet velocity (by anemometer)	
	Air temperatures of outside, attic space, and crawl space (by anemometer)	
	Electric consumption of system (by wattmeter)	

Table 4. Basic Equations.

$$\frac{\partial U_i}{\partial x_i} = 0$$

$$\frac{\partial U_i}{\partial t} = -\frac{\partial U_i U_j}{\partial x_j} - \frac{\partial \pi}{\partial x_i} + \frac{\partial}{\partial x_j}\left\{(\nu_t + \nu)\left(\frac{\partial U_i}{\partial x_j} + \frac{\partial U_j}{\partial x_i}\right)\right\} \quad (1)$$

$$\frac{\partial k}{\partial t} = -\frac{\partial k U_j}{\partial x_j} + \nu_t\left(\frac{\partial U_i}{\partial x_j} + \frac{\partial U_j}{\partial x_i}\right)\frac{\partial U_i}{\partial x_j} + \frac{\partial}{\partial x_j}\left\{\left(\frac{\nu_t}{\sigma_k} + \nu\right)\frac{\partial k}{\partial x_j}\right\} - \varepsilon \quad (2)$$

$$\frac{\partial \varepsilon}{\partial t} = -\frac{\partial \varepsilon U_j}{\partial x_j} + c_{\varepsilon 1}\frac{\varepsilon}{k}\nu_t\left(\frac{\partial U_i}{\partial x_j} + \frac{\partial U_j}{\partial x_i}\right)\frac{\partial U_i}{\partial x_j} + \frac{\partial}{\partial x_j}\left\{\left(\frac{\nu_t}{\sigma_\varepsilon} + \nu\right)\frac{\partial \varepsilon}{\partial x_j}\right\} - c_{\varepsilon 2}\frac{\varepsilon^2}{k} \quad (3)$$

$$\frac{\partial \theta}{\partial t} = -\frac{\partial \theta U_j}{\partial x_j} + \frac{\partial}{\partial x_j}\left\{\left(\frac{\nu_t}{\sigma_\theta} + \nu\right)\frac{\partial \theta}{\partial x_j}\right\} \quad (4)$$

$$\nu_t = c_D\frac{k^2}{\varepsilon} \quad (5) \qquad \pi = \frac{P}{\rho} + \frac{2}{3}k \quad (6)$$

$$\sigma_k = 1.0, \quad \sigma_\varepsilon = 1.3, \quad \sigma_\theta = 1.0, \quad c_{\varepsilon 1} = 1.59, \quad c_{\varepsilon 2} = 2.0, \quad C_D = 0.09$$

[Nomenclature]

U_i : Velocity in i's direction
P : Pressure
k : Turbulent energy
ε : Dissipation of k
ν_t : Effective eddy viscosity
θ : Temperature
ρ : Density
ν : Viscosity of air
t : Time
x_i : i's direction

Table 5. Boundary conditions.

Wall Boundary condision for U, k, ε

$$\left.\frac{\partial U}{\partial y}\right|_{wall} = \frac{1}{7}\frac{U_p}{y_p}, \qquad \left.\frac{\partial k}{\partial y}\right|_{wall} = 0, \qquad \varepsilon_p = \frac{C_D^{\frac{3}{4}} k^{\frac{3}{2}}}{\kappa y_p} \tag{1}$$

Wall Boundary condision for θ

$$q_w = \alpha\left(\theta_p - \theta_w\right) \tag{2}$$

$$\alpha = 5.3 + 3.6\overline{U_p} \tag{3}$$

$$\left.\frac{\partial \theta}{\partial y}\right|_{wall} = \frac{1}{7}\frac{\theta_p - \theta_w}{y_p} \tag{4}$$

Boundary condision of outlet

$$U_{out},\ \theta_{out}: \text{Measured value},\ k_{out} = 0.005,\ \varepsilon_{out} = \frac{C_D k_{out}^{\frac{2}{3}}}{l_{out}},\ l_{out} = 0.05 \tag{5}$$

Boundary condision of intlet

$$U_{out}: \text{Balanced values to outlet},\ \left.\frac{\partial k}{\partial y}\right|_{in} = 0,\ \left.\frac{\partial \varepsilon}{\partial y}\right|_{in} = 0,\ \left.\frac{\partial \theta}{\partial y}\right|_{in} = 0 \tag{6}$$

[Nomenclature]

κ : von Karman's constant

q_w : heat flux on an inside surface

α : Inside film coefficient

θ_w : Wall surface temperature

$\overline{U_p}$: Conposition velocity lateral the wall

l_{out} : Turbulent length at outlet

y_p : distance from the wall to a node adjacent to the wall,

subscript of p : Values at a node adjacent to the wall

subscript of *out* : Values at a outlet

subscript of *in* : Values at a inlet

Table 6. Heat supply from air-conditioner (Experiment & Simulation).

	Case1	Case2	Case3	Case4
Temperature (°C)				
Outlet (Experimental value)	38.2	36.9	37.0	36.3
Inlet (Experimental value)	24.7	23.2	23.5	23.0
Inlet (Calculated value)	23.0	22.0	22.4	22.5
Average room temperature (°C)				
Experimental value	22.7	21.7	21.9	21.2
Calculated value	21.9	21.6	21.8	21.5
Heat supply (kW)				
Experimental value	1.99	2.02	1.99	1.96
Calculated value	2.16	2.11	2.06	1.96

Table 7. Heat losses.

	Case1	Case2	Case3	Case4
Experimental result(kW).				
Wall-1	0.725	0.750	0.666	0.691
Wall-2	0.071	0.067	0.072	0.069
Wall-3	0.543	0.504	0.514	0.641
Wall-4	0.048	0.048	0.045	0.042
Floor	0.192	0.193	0.232	0.229
Ceiling	0.132	0.128	0.113	0.118
Ventilation	0.190	0.180	0.177	0.177
Total(experiment)	1.091	1.870	1.819	1.967
Calculated result(kW).				
Total(Calculation)	2.069	1.965	1.921	1.881

Table 8. Normalized heat losses (experiment : kW).

	Case1	Case2	Case3	Case4
Wall-1	0.694	0.758	0.683	0.735
Wall-2	0.068	0.068	0.074	0.073
Wall-3	0.519	0.509	0.528	0.687
Wall-4	0.046	0.048	0.046	0.045
Floor	0.237	0.230	0.254	0.260
Ceiling	0.130	0.133	0.119	0.129
Ventilation	0.182	0.182	0.182	0.182
Total	1.876	1.928	1.886	2.121